Basin-to-shelf correlations in the Canning Basin, NW Australia, using Stable Carbon Isotope Stratigraphy

By
James D. Griffiths (Chemostrat Ltd.)[1]
Nicholas B. Sullivan (Chemostrat Inc.)
Meg Long (Chemostrat Australia Pty.)
Andy Wilson (Chemostrat Australia Pty.)*
Ken Ratcliffe (Chemostrat Ltd.)

1 Corresponding author: jamesgriffiths@chemostrat.com *Now at Taskfronterra Geosciences

ABSTRACT

Stable isotope stratigraphy (SIS) was used to place two wells from the Canning Basin, NW Australia, into a global chronostratigraphic context. A stable carbon isotope record was reconstructed for the Mississippian (ff360-323 Ma, Lower Carboniferous) Fairfield Group from the Yulleroo-4 and Ungani-2 wells, and compared to global published isotope records for the same interval.

Robust isotopic global correlative ties for the Canning Basin wells were established to records from Nevada, Belgium and China. These correlations are supported by independent biostratigraphy and reveal that the Canning Basin experienced significant palaeoenvironmental change during the Mississippian.

INTRODUCTION

Chronostratigraphy is a key consideration in hydrocarbon exploration. The determination of when particular events occurred in the geological past can have important implications for understanding depositional history and resource distribution. A robust chronostratigraphic framework aids subsurface stratigraphic correlation and characterisation of geological units. One way of correlating complex facies is to use stable-isotope stratigraphy (e.g. Scholle & Arthur, 1980; Koch et al., 1992; 2014).

The Canning Basin is a large intracratonic basin that ranges in age from Ordovician to Cretaceous, although it predominantly comprises Paleozoic strata. It is the largest basin in Western Australia, with an onshore area of ff530,000 km^2 and an offshore area of ff110,000 km^2. It hosts four active petroleum systems, and has exhibited hydrocarbon shows at many stratigraphic levels (e.g. Apak & Carlsen, 1997, Haines, 2004; Haines & Ghori, 2006).

A report by the US Energy Information Agency in 2013 indicated that the Canning Basin hosts the largest unconventional potential in Australia, and the eighth largest in the world, with in excess of 225 TCF of recoverable shale gas based on the Middle Ordovician Goldwyer Formation alone (WA Govt. Dept. Mines and Petroleum Report, 2014).

Currently, the Canning Basin has a very low well density (four wells/10,000 km^2, as of February 2014) compared to the Paleozoic basins of North America which average 500 wells/10,000 km^2. Further exploration in the basin could be highly successful based on the presence of five discovered oilfields, new gas discoveries, many and varied petroleum shows and huge shale gas potential. Established pathways to market exist in the region, including a refinery in the Perth metropolitan area and export facilities at the port of Broome.

There are several conventional and unconventional hydrocarbon plays being targeted in the Canning Basin, and are summarised in the table below on the following page.

The Early-Middle Mississippian (ff359-323 Ma) carbonate-shale Fairfield Group contains both conventional and unconventional hydrocarbon plays; with the conventional plays located in the deeper water depositional system of the Fitzroy Trough and the unconventional carbonate plays being age-equivalent shallow marine platform carbonates. Understanding the relationship between these two depositional systems presents an enormous correlation problem. This is compounded by weak biostratigraphic control, based on the Ungani-1 well which is adjacent

TABLE 1 – Key plays in the Canning Basin with potential analogues (WA Govt. Dept. Mines and Petroleum Report, 2014).

Age	Play	International analogues
Conventional		
Permian	Worral Fm. - Grant Gp. suprasalt sombrero dissolution features	Eastern flank of South Oman Salt Basin, giant oilfields
Permian-Carboniferous	Grant Group, clastics	Unayzah Fm., Saudi Arabia; Oman
Early Carboniferous	Laurel Fm., dolomites	Dnieper-Donets Basin, Ukraine
Devonian	Lennard Shelf carbonate reefs (stratigraphic traps)	Alberta Basin giant oilfields, Canada
Silurian-Ordovician	Carribuddy Gp. Goldwyer Fm. Nita Fm.	Late Carboniferous Paradox Basin, US
Ordovician	Fractured Nita and Goldwyer Fms. Nita Fm. Dolomite and Upper Willara Fm., carbonate Nambeet Fm., sandstone	W. Texas Cambrian-Ordovician Ellenburger Dolomite, giant gasfields Dolomite reservoirs, e.g. prolifically producing Red River Fm, Williston Basin Possibly Sirte Basin, Libya, giant gasfields and Murzuk Basin, Libya, giant oilfields
Paleozoic	Truncated reservoirs, base Permian unconformity	
Unconventional		
Carboniferous	Laurel Fm., tight gas Laurel Fm., BCGA	Barnett Shale, US Dnieper-Donets Basin, Ukraine
Devonian	Gogo Fm., shale gas	Marcellus Shale, US
Ordovician	Goldwyer Fm., shale gas and shale oil	Utica Shale, Bakken Shale, US and Canada

to Ungani-2. The interval 2085-2280 m in Ungani-1 has been aged as late Famennian (Upper Devonian) or younger based on the palynomorph R. lepidophyta. Obtaining further biostratigraphic data is often expensive, time-consuming and requires large samples (>0.5 kg).

The purpose of this study was to use Stable Isotope Stratigraphy (SIS) to aid well-to-well correlation and provide chronostratigraphic context for two onshore wells (Yulleroo-4 and Ungani-2) from the Canning Basin. This was achieved through the creation of a stable carbon isotope record spanning the Lower Carboniferous (Mississippian) chronostratigraphic interval of both wells, and comparing the data to published global records.

SAMPLING LOCATIONS AND ANALYSES

The Yulleroo-4 well is located in the southern part of the Fitzroy Trough, in the onshore portion of the Canning Basin, around 80 kilometres to the east of Broome (Fig. 1). The Ungani-2 well is located around 45 kilometres to the southeast of Yulleroo-4 (Fig. 1). From Yulleroo-4, 101 claystone/silty claystone cuttings samples were analysed for $\delta^{13}C_{org}$; from Ungani-2, 20 cuttings samples were analysed for $\delta^{13}C_{org}$, 14 calcite cuttings samples, and 16 dolomite cuttings samples were analysed for $\delta^{13}C_{carb}$. The sample depth ranges for Yulleroo-4 were 2340-3846 m and 2400-2675 m for Ungani-2.

The cuttings samples were cleaned, then 'picked' to make sure that they were truly representative of the surrounding lithology. Picking involved technicians selecting samples from cuttings material based on the well gamma log, selecting material "typical" of the interval and avoiding nodules, lags, rip-ups, larger clasts and obvious diagenetic features. Claystones required a 2cm^3 chip for analysis, with carbonates requiring a smaller amount.

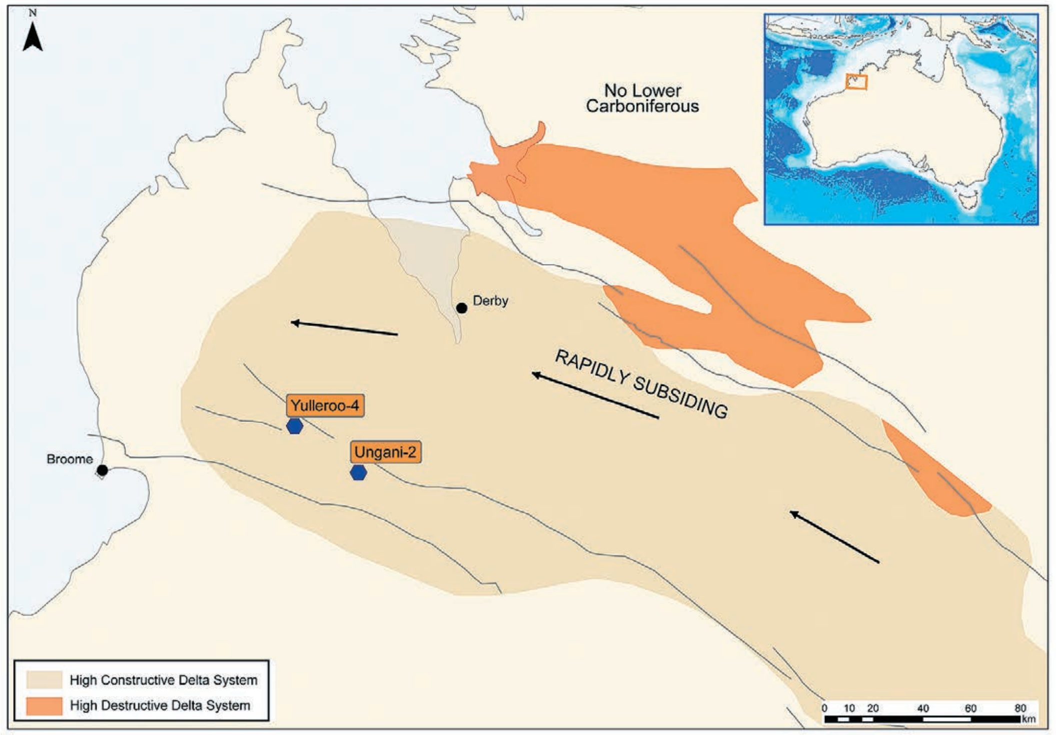

Figure 1: *Map of the Canning Basin showing the palaeo-depositional system for the Mississippian Lower Laurel Formation Carbonates. The location of the study wells Yulleroo-4 and Ungani-2 are shown within the context of the Lower Carboniferous delta facies. Dark lines are major fault planes.*

Source: *Buru Energy.*

The effectiveness of the sample picking was tested by creating a 'synthetic' gamma log, based on the amount of potassium (K), thorium (Th) and uranium (U); and is termed chemical gamma ray (CGR). CGR is calculated as follows and approximates the wireline gamma log response (Ellis & Singer, 2007):

CGR = (K x 16.32 x 0.83) + (Th x 3.93) + (U x 8.09)

The CGR for each interval was compared to the wireline gamma log, and where it matches well the picked lithology was considered representative of the interval. Samples were then washed, ground to a (<63 μm) powder. Bulk rock sample powders were then analysed to determine their carbon isotopic composition (see Analytical Methods below).

METHODOLOGY AND STABLE ISOTOPE STRATIGRAPHY BACKGROUND

Stable carbon isotope stratigraphy utilises the difference in the stable isotopic composition of kerogen in shale/mudstone/marl ($\delta^{13}C_{org}$) or bulk calcium carbonate ($\delta^{13}C_{carb}$). The ratio of the heavy isotope carbon-13 (13C) to the light isotope carbon-12 (12C) in a given material is expressed as a decimal value in the per mille (‰) notation, and is calculated using the equation below:

$$\delta^{13}C = \left(\frac{\left(\frac{^{13}C}{^{12}C}\right)_{sample}}{\left(\frac{^{13}C}{^{12}C}\right)_{standard}} - 1 \right) \times 100\ ‰$$

Equation 1

The stable isotope composition of a material is measured relative to an international standard termed the Vienna Pee Dee Belemnite (VPDB). This is an artificial standard, based on the original isotopic standard, the Pee Dee Belemnite. This standard was based in turn on a Cretaceous marine fossil with an anomalously high 13C:12C ratio of 0.0112372, which was established as a $\delta^{13}C$ value of zero (Craig, 1957).

Although the precise controls on $\delta^{13}C$ are disputed, it is generally agreed that they are intimately linked with the burial rate of organic carbon. Photosynthetic microorganisms preferentially take up lighter 12C as it requires marginally less energy to absorb and incorporate into biochemical reactions. This means that $\delta^{13}C_{org}$ is enriched in 12C relative to $\delta^{13}C_{carb}$, as kerogen in organic matter is ff -25 ‰ lighter than calcium carbonate (limestone and dolomite). Calcium carbonate is precipitated from the global oceanic reservoir of dissolved inorganic carbon (DIC) which has an isotopic value of ffO ‰ (Hoefs, 2009).

When microorganisms die, and organic carbon is buried, this leads to depletion in 12C and a consequent increase in $\delta^{13}C$ values of subsequently-deposited sediments. When samples from these strata are analysed in the course of exploratory drilling, their $\delta^{13}C$ value reflects palaeoenvironmental conditions and can give information on organic carbon burial rates in the geological past.

The $\delta^{13}C$ patterns in stratigraphic successions are isochronous and traceable over vast distances (e.g. Munnecke et al., 2003; Yans et al., 2007; Sliwinski et al., 2011; Pisarzowska & Racki, 2012). Moreover, $\delta^{13}C$ values in marine sedimentary rocks are very resistant to late diagenetic alteration, and are largely uncontrolled by facies (McLaughlin et al., 2012). The compilation of large published $\delta^{13}C$ datasets from almost every global region have been linked to the geologic timescale, which establishes the isochronous nature of global $\delta^{13}C$ excursions and carbon isotope events (CIEs; Saltzman and Thomas, 2012). This then allows newly-acquired isotopic data to be placed in a global chronostratigraphic context. An example of a global carbon isotope excursion can be found in the Upper Devonian (Frasnian) punctata conodont biozone (see Fig. 2).

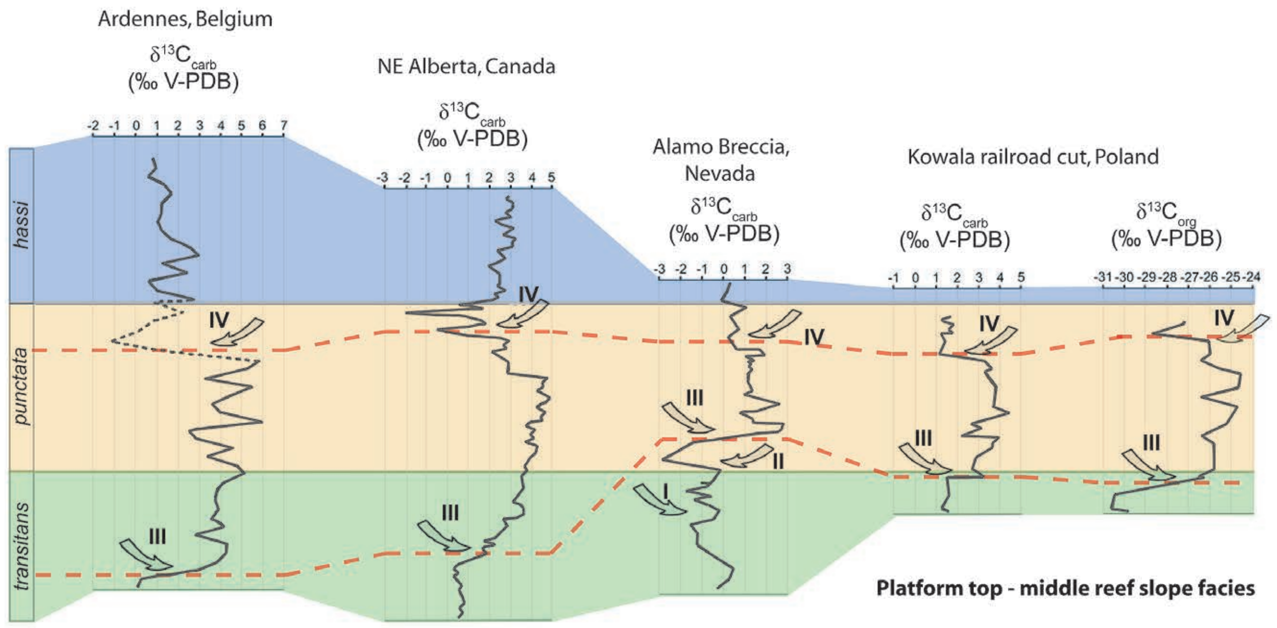

Figure 2: *A plot of carbon isotope records from a variety of global locations and geological settings (Holmden et al., 2006; Yans et al., 2007; Morrow et al., 2009; Pizarzowska & Racki, 2012). The plot emphasises the coherent nature of the steps within the Middle Frasnian isotopic excursions marked 'Event III' and 'Event IV'. The carbon isotope excursion occurs approximately coeval with the conodont punctata biozone, and is recognised as a global event (Holmden et al., 2006; Yans et al., 2007; Ma et al., 2008; Morrow et al., 2009; Śliwiński et al. 2011; Pizarzowska & Racki, 2012). Note that excursions are recorded in the organic carbon isotopic record (Kowala, Poland - far right) as clearly as in the carbonate record. The conodont biostratigraphy provides an independent chronostratigraphic framework. Figure modified from Pizarzowska & Racki, 2012*

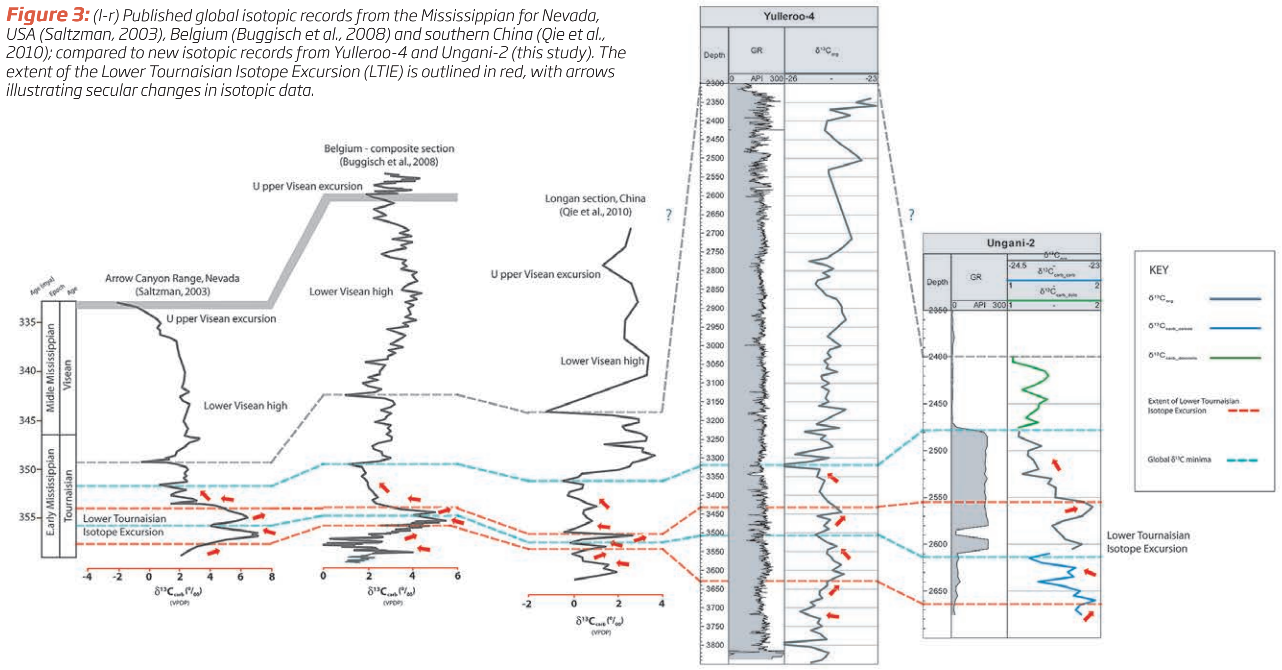

Figure 3: *(l-r) Published global isotopic records from the Mississippian for Nevada, USA (Saltzman, 2003), Belgium (Buggisch et al., 2008) and southern China (Qie et al., 2010); compared to new isotopic records from Yulleroo-4 and Ungani-2 (this study). The extent of the Lower Tournaisian Isotope Excursion (LTIE) is outlined in red, with arrows illustrating secular changes in isotopic data.*

ANALYTICAL METHODS – ORGANIC-RICH FACIES ($\delta^{13}C_{org}$)

Sample Preparation (carbonate removal): Weighed sub-samples were acidified with 2M hydrochloric acid, mixed, oven heated at 60 °C for 2 hours and left for 24 hours to allow all carbonate to be liberated as CO_2. The acidified samples were then isolated by centrifugation and the acid was then decanted. The samples were then washed twice using distilled water and centrifugation. After acid washing, the fractions were oven dried at 60 °C. After drying, the samples were re-ground in-situ. The samples were then analysed using an Elemental Analyser-Isotope Ratio Mass Spectrometer (EA-IRMS).

ANALYTICAL METHODS – CALCIUM CARBONATE ($\delta^{13}C_{carb}$)

Samples were weighed into clean Exetainer™ tubes and the tubes placed in a drying oven for 24 hours to remove moisture. Once the samples were dry, septum caps were fitted to the tubes. The tubes were then flushed and filled with helium. Acid was added to the samples and they were allowed to react for 24 hours then heated to 60° C for 2 hours to allow complete conversion of carbonate to CO_2.

The CO_2 gas liberated from samples was then analysed by Continuous Flow-Isotope Ratio Mass Spectrometry (CF-IRMS).

STABLE CARBON ISOTOPE RECORD FOR THE LOWER CARBONIFEROUS (MISSISSIPPIAN) FAIRFIELD GROUP

Results are displayed in Figure 3. Shown on the left of Figure 3 is a $\delta^{13}C_{carb}$ dataset for the Mississippian Stage of the Carboniferous Period from the Arrow Canyon Range in Nevada, USA (Saltzman, 2003), a composite Mississippian $\delta^{13}C_{carb}$ record from Belgium (Buggisch et al., 2008), and a Mississippian record from the Yangtze Platform, southern China (Qie et al., 2010). This section was selected for comparison to the Australian study wells as the south China block was situated adjacent to the Australian palaeo-continent on the south eastern flank of the Palaeo-Tethys Sea (Blakey, 2010) (see Fig. 5).

The Yulleroo-4 and Ungani-2 isotopic datasets are compared to these biostratigraphically-constrained published isotopic datasets, in order to place the samples in chronostratigraphic context. There is a ~25 ‰ offset between $\delta^{13}C_{org}$ and $\delta^{13}C_{carb}$ which is evident in the Ungani-2 datasets below. This offset can be considered more or less constant, as the $\delta^{13}C$ values from both marine carbonate and organic matter are closely linked to the global carbon reservoir; meaning that CIEs are recorded in limestones as well as shales and mudstones (Hoefs, 2009). However, the relationship between the stable isotopic compositions of marine carbonate and organic matter is complex, and has varied over geological time (Hayes et al., 1999; Kump & Arthur, 1999). Therefore it should be considered qualitative rather than quantitative. The scale for the $\delta^{13}C_{org}$ record in Ungani-2 is offset by 25 ‰ in Figure 3 to allow an approximate comparison of isotopic data with carbonate/dolomitic lithologies. This study also demonstrates that composited datasets can be made from calcitic ($\delta^{13}C_{carb}$), dolomitic ($\delta^{13}C_{carb}$) and shale/marl samples ($\delta^{13}C_{org}$); which can then be correlated to global isotopic datasets (left of Fig. 3).

A major (~5-6 ‰) positive carbon isotopic excursion occurs during the Lower Tournaisian (Early Mississippian, ~359-347 Ma) in the published North American isotopic dataset (Saltzman et al., 2003) and the Belgian dataset (Buggisch et al., 2008). There is a concurrent 2 ‰ positive excursion in the Chinese dataset (Qie et al., 2010). These data are used to place the samples from Yulleroo-4 and Ungani-2 in a global chronostratigraphic outline (Fig. 3). In Yulleroo-4 this positive excursion ('Lower Tournaisian Isotope Excursion') occurs between ~3440 and 3625 m; and in Ungani-2 it occurs between ~2550 and 2660 m. Identification of the Tournaisian isotopic excursion is based on the pattern of secular trends in the isotopic data, rather than the absolute magnitude of the excursions, as slight diagenetic alteration, or differences in depositional water depth may 'dampen' the magnitude of the excursion by up to 2 ‰, whilst leaving its form unaltered (Brenchley et al., 2003).

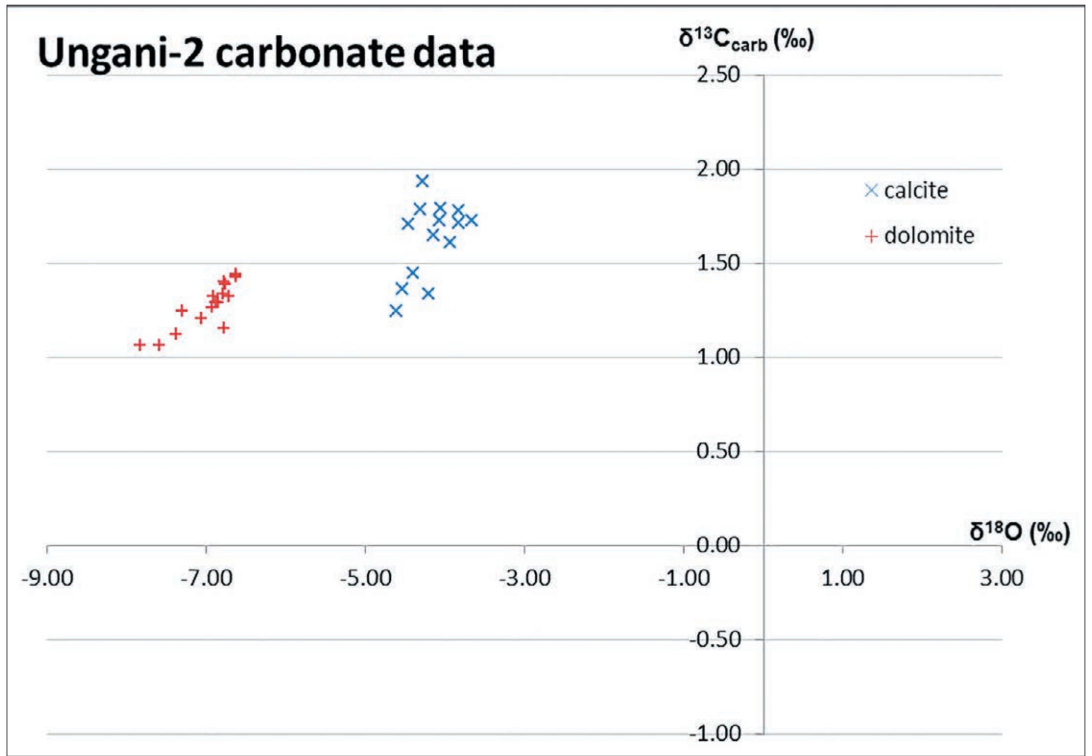

Figure 4: *Cross plot of $\delta^{13}C_{carb}$ data and δ18O data from the Ungani-2 well. These data show that the Ungani-2 sequence has been minimally affected by diagenetic alteration in terms of meteoric water diagenesis, although the dolomitised interval has been more affected by burial diagenesis than the (calcitic) carbonate section. Diagenetic alteration has affected only the δ18O values, and not the $\delta^{13}C_{carb}$; therefore late diagenetic alteration is not likely to have affected the chronostratigraphic correlation in this case.*

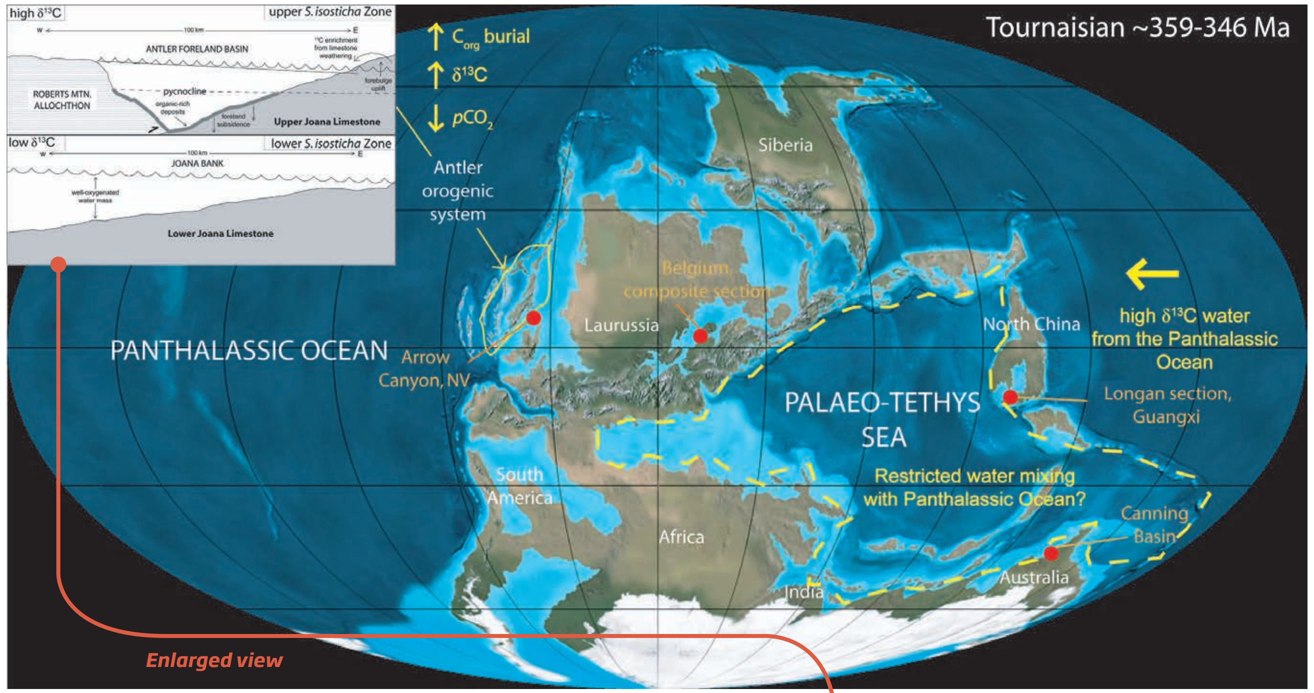

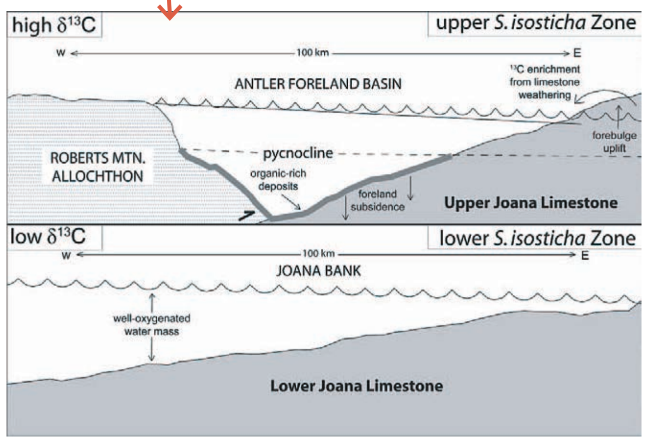

Figure 5: *Palaeogeographic map of Earth during the Tournaisian (Mississippian/Lower Carboniferous) (Blakey, 2010). The inset shows the proposed mechanism for enhanced organic carbon burial in the Antler Foreland Basin, which may have initiated a glacial episode during the Tournaisian (Saltzman et al., 2000). This would have led to a positive $\delta^{13}C$ excursion which is seen globally (e.g. Saltzman et al., 2000; Buggisch et al., 2008; Qie et al., 2010). A possible reason for the reduced magnitude of the lower Tournaisian positive isotopic excursion in the southern China and Canning Basin datasets may be due to restricted mixing between the Panthalassic Ocean and the closing Palaeo-Tethys Sea. This may have affected nutrient availability and constrained organic carbon burial in this region, in contrast to the high organic carbon burial rates seen in the Nevada and Belgian datasets, from Laurussia (Saltzman et al., 2000; Buggisch et al., 2008). Locations of all chronostratigraphic comparison datasets are shown in orange.*

The Chinese Mississippian isotope record shows a reduced amplitude lower Tournaisian isotope excursion (relative to the positive isotopic excursion in the upper Tournaisian), in comparison to the Arrow Canyon and Belgian datasets. This is probably due to differences in the palaeogeographic setting (the Longan section is a deeper isolated carbonate platform), and/or the burial velocity of organic carbon in the different regions (Qie et al., 2010). However, independent biostratigraphy places this excursion in the Lower Tournaisian, in the upper S. crenulata-S. isosticha conodont biozone; which is the same biozone as that in which a major positive excursion takes place in the Mississippian (Kinderhookian) sections from Nevada (Saltzman et al., 2000; Saltzman, 2003; Qie et al., 2010).

The top of the Laurel Formation in Yulleroo-4 has been placed at 2483 m by Buru Energy. The pattern of $\delta^{13}C_{org}$ excursion suggests that the Lower Visean high occurs in Yulleroo-4 from upwards of ~2780 m, although there are some sample gaps in the upper part of the record. There is a possible unconformity separating the Laurel Formation from the Visean age Anderson Formation (WA Govt. Dept. Mines and Petroleum Report, 2014).

However, it is important to note that the onset of the positive CIE which marks the Lower Visean high actually occurs within the uppermost Tournaisian, which is consistent with the datasets from Nevada (Saltzman, 2003), Belgium (Buggisch et al., 2008) and China (Qie et al., 2010). This places the top of the Laurel Formation in the uppermost Tournaisian.

Palynomorph biostratigraphy from the Ungani-1 well suggests an age of Famennian (Upper Devonian) for the Fairfield Group, of which the Laurel Formation is a part. However, the pattern of isotopic variation in Ungani-2 shows a trend towards a $\delta^{13}C_{carb}$ minimum in the proposed upper Tournaisian (the uppermost dashed blue line in Fig. 3), which is a common feature with all the other published datasets. The upper part of the Famennian, by contrast, trends towards more positive $\delta^{13}C_{carb}$ values. This short-lived event is identified globally as the Hangenburg Event, and is coincident with widespread black shale deposition (House 2002; Kaiser 2009; Myrow, 2011; 2013; 2014). The

Hangenburg Event has been precisely dated from a section in Poland, and lasted 50-100 ka (Myrow, 2014). By contrast, the LTIE lasts ~9 Ma. The sedimentation rate in Yulleroo-4 is approximately 4 cm/ka, and as this rate the Hangenburg would only be ~2 m in thickness which precludes it from being the positive isotopic excursion in the lower parts of Yulleroo-4 and Ungani-2. Therefore, the carbon isotope stratigraphic data from Ungani-2 place the uppermost data point (at ~2400 m) as upper Tournaisian, immediately prior to the Lower Visean positive CIE.

A cross-plot of the $\delta^{13}C_{carb}$ and $\delta^{18}O$ values (Fig. 4) shows a slight diagenetic influence of burial on the Ungani-2; however this affects only the $\delta^{18}O$ values and leaving the $\delta^{13}C_{carb}$ values relatively unaltered from the standard marine values of ~-1 to 3 ‰ (Hoefs, 2009).

The amplitude of the excursions in the $\delta^{13}C_{org}$ record from Yulleroo-4 are significantly 'damped' relative to the clear excursions in Ungani-2. However, the pattern of secular changes are the same, and suggest that the lower part of the record is Tournaisian (trending towards a $\delta^{13}C_{org}$ minimum in the upper Tournaisian – upper blue dashed line in Fig.3), which rules out the upper Famennian as the trend is in the opposite direction.

DISCUSSION

Carbon isotope excursions (CIEs) in the geological past are thought to be caused by reduced marine primary productivity, and/or increased organic matter burial (Arthur et al., 1987; Kump & Arthur, 1999). The events which lead to these changes in organic matter burial rates are not always well understood, but probably depended on many factors, including temperature, oceanic circulation, tectonic influence/ sea level and redox conditions (Munnecke et al, 2003; Saltzman & Thomas, 2012).

The distinct positive CIE seen in the base of the Tournaisian in this Canning Basin isotopic dataset was probably a global event, and may have been driven by events on the palaeocontinent Laurussia (Saltzman & Lohmann, 2000; Saltzman, 2002; 2003). The proposed mechanism is that rapid subsidence of the Joana platform (upper Kinderhookian marine carbonate, Tournaisian age-equivalent) within the Antler Foreland Basin led to enhanced organic carbon burial rates in response to tectonic deepening. Subsequently this created a restricted deep water mass in the Antler foredeep and other foredeeps of similar age, and led to widespread organic matter preservation below the pycnocline (Saltzman et al., 2000). This series of events drew down atmospheric CO_2 (pCO_2) and was probably one of the contributing factors to the Late Paleozoic (~355-255 Ma) glaciation (Veevers & Powell, 1987; Saltzman, 2003, Montañez et al., 2007).

Therefore, the event is strongly expressed in the carbon isotope record from Nevada (Saltzman, 2003) and Belgium (Buggisch et al., 2008), which were both part of the palaeocontinent Laurussia on the western side of the Palaeo-Tethys Sea (see Fig. 5). This major carbon isotope excursion is also recorded in other sections from Europe, mid-continent USA and the Russian Platform (Mii et al., 1999; Saltzman et al., 2000; Mii et al., 2001; Buggisch et al., 2008; Grossman et al., 2008). This hypothesis is supported by a positive shift in conodont $\delta^{18}O$ from Belgium, suggesting global cooling during the lower Tournaisian (Buggisch et al., 2008).

The lower Tournaisian isotopic excursion is also seen in the Longan section, from Guangxi in southern China (Qie et al., 2010). During the lower Carboniferous, the south China block was situated adjacent to Australia on the south-eastern side of the Palaeo-Tethys Sea. Similar to the Longan section, the Fairfield Group of the Canning basin was deposited in the northern part of the basin; on the Lennard Shelf, the Fitzroy Trough and the Jurgarra Terrace (Druce & Radke, 1979). The calcium carbonate and kerogen deposited in the Canning basin during the lower Tournaisian was sourced from the same oceanic carbon reservoir, which was responding to global cooling and glaciation. These global palaeoclimatic changes influenced the isotopic composition of both the organic and inorganic global carbon reservoirs, and led to the expression of a positive carbon isotopic excursion in the Canning basin during the lower Tournaisian (see Fig. 5).

A possible reason for the lower amplitude of the lower Tournaisian excursion in the Canning Basin may be due to the reorganisation of continents and the redistribution of global oceanic nutrients (Saltzman, 2003). During the Mississippian the Palaeo-Tethys Sea was ringed by islands, which may have restricted nutrient input (and therefore reduced organic carbon burial) in the Canning Basin during the Mississippian (see Fig. 5).

CONCLUSIONS

The use of Stable Isotope Stratigraphy (SIS) on samples from the Canning Basin, north Western Australia has demonstrated that the technique aids stratigraphic correlation. The use of SIS has revealed a robust correlative tie between the Yulleroo-4 and Ungani-2 wells in the Lower Tournaisian (Mississippian, ~359-347 Ma). This dataset has also allowed the Canning Basin intervals to be placed in a global stratigraphic context, based on comparison with published records from North America, Belgium and China. These data show that the Canning Basin was influenced by global changes in the oceanic carbon reservoir during the Mississippian (Lower Carboniferous) between ~360 and 330 Ma.

ACKNOWLEDGEMENTS

The authors gratefully acknowledge the assistance of Buru Energy and Mitsubishi Corporation in obtaining sample material for this investigation. Our thanks also go to Maja Buschkuehle for her input to the manuscript.

TECH TALK

REFERENCES

APAK, SN AND CARLSEN, GM 1997, A compilation and review of data pertaining to the hydrocarbon prospectivity of the Canning Basin: Geological Survey of Western Australia, Record 1996/10,103p.

ARTHUR, M. A., SCHLANGER, S. O. AND JENKYNS, H. C., 1987. The Cenomanian-Turonian oceanic anoxic event. II. Palaeoceanographic controls on organic matter production and preservation. In: Brooks, J., Fleet, A. J. (Eds.), Marine Petroleum Source Rocks. Geological Society of London Special Publication, 26: 401-420.

BLAKEY, R.C, 2010. Library of Paleogeography at www.cpsgeosystems.com.

BRENCHLEY, P. J., CARDEN, G. A., HINTS, L., KALJO, D., MARSHALL, J. D., MARTMA, T., MEIDLA, T. AND NÕLVAK, J., 2003. High-resolution stable isotope stratigraphy of Upper Ordovician sequences: Constraints on the timing of bioevents and environmental changes associated with mass extinction and glaciation. Geological Society of America Bulletin, 115(1):89-104.

BUGGISCH, W., JOACHIMSKI, M. M., SEVASTOPULO, G. AND MORROW, J. R., 2008. Mississippian $\delta^{13}C_{carb}$ and conodont apatite $\delta^{18}O$ records – Their relation to the Late Palaeozoic Glaciation. Palaeogeography, Palaeoclimatology, Palaeoecology 268:273–292.

COPLEN, T. B., KENDALL, C. AND HOPPLE, J., 1983. Comparison of stable isotope reference samples, Nature, 302: 236-238.

CRAIG, H., 1957. Isotopic standards for carbon and oxygen and correction factors for mass-spectrometric analysis of carbon dioxide. Geochmica et Cosmochimica Acta, 12: 133-149.

DRUCE, E.C. AND RADKE, B.M., 1979. The geology of the Fairfield Group, Canning Basin, Western Australia. Bulletin 200. Bureau of Mineral Resources, Geology and Geophysics, Canberra.

ELLIS, D.V. AND SINGER, M. (2007). Well logging for Earth Scientists. Springer Science + Business Media B.V. 692pp.

Government of Western Australia Department of Mines and Petroleum (Petroleum Division), 2014. Summary of Petroleum Prospectivity: Canning Basin.

HAINES, PW 2004, Depositional facies and regional correlations of the Ordovician Goldwyer and Nita Formations, Canning Basin, Western Australia, with implications for petroleum exploration: Geological Survey of Western Australia, Record 2004/7, 45p.

HAINES, PW AND GHORI, KAR 2006, Rich oil-prone Ordovician source beds, Bongabinni Formation, onshore Canning Basin, Western Australia, in Extended Abstracts: American Association of Petroleum Geologists; AAPG International Conference and Exhibition, Perth, Western Australia, 5 November 2006, 4p.

HOEFS, J., 2009. Stable Isotope Geochemistry. 6th ed., Springer-Verlag, Berlin Heidelburg, pp 285.

HOLMDEN, C., BRAUN, W.K., PATTERSON, W.P., EGLINGTON, B.M., PROKOPIUK, T.C., WHITTAKER, S., 2006. Carbon isotope chemostratigraphy of Frasnian sequences in western Canada. Summary of Investigations 2006, Volume 1, Saskatchewan Geological Survey, Sask: Industry Resources, Misc. Rep. 2006–4.1, CD-ROM, Paper A-8: 1–6.

HOUSE, M. R., 2002. Strength, timing, setting and cause of mid-Paleozoic extinctions. Palaeogeography, Palaeoclimatology, Palaeoecology, 181: 5-25.

KAISER, S. I., BECKER, R. T., SPALETTA, C. AND STEUBER, T., 2009. High-resolution conodont stratigraphy, biofacies, and extinctions around the Hangenburg Event in pelagic successions from Austria, Italy and France. In: Over, D. J. (Ed., Studies in Devonian Stratigraphy: Proceedings of the 2007 International Meeting of the Subcommission on Devonian Stratigraphy and IGCP 499: Paleontographica Americana, 63: 97-139.

KOCH, P.L., ZACHOS, J.C., AND GINGERICH, P.D., 1992. Correlation between isotope records in marine and continental carbon reservoirs near the Palaeocene/Eocene boundary. Nature 358: 319-322.

KOCH, J.T., FRANK, T.D. AND BULLING, T.P., 2014. Stable-isotope chemostratigraphy as a tool to correlate complex Mississippian marine carbonate facies of the Anadarko shelf, Oklahoma and Kansa. American Association of Petroleum Geologists, Bulletin. 98: 1071-1090.

KUMP, L. R. AND ARTHUR, M. A., 1999. Interpreting carbon-isotope excursions: carbonates and organic matter. Chemical Geology, 161: 181-198.

MA, X.P., WANG, C.Y., RACKA, M., RACKI, G., 2008. Isotope and inorganic geochemistry across the Early–Middle Frasnian transition (Late Devonian) on South China carbonate shelf: comparison with the Polish reference. Palaeogeography, Palaeoclimatology, Palaeoecology 269: 130–151.

McLAUGHLIN, P.I., EMSBO, P., AND BRETT, C.E. 2012. Beyond black shales: the sedimentary and stable isotope records of oceanic anoxic events in a dominantly oxic basin (Silurian; Appalachian Basin, USA). Palaeogeography, Palaeoclimatology, Palaeoecology, 367-368: 153-177.

MII, H., GROSSMAN, E.L., YANCEY, T.E., 1999. Carboniferous isotope stratigraphies of North America: Implications for Carboniferous paleoceanography and Mississippian glaciation. Geological Society of America Bulletin, 111: 960-973.

MII, H., GROSSMAN, E.L., YANCEY, T.E., CHUVASHOV, B., AND EGOROV, A., 2001, Isotope records of brachiopod shells from the Russian platform—Evidence for the onset of mid-Carboniferous glaciation: Chemical Geology, 175: 133–147. Montañez, I. P., DiMichele, W. A., Isbell, J. L., Tabor, N. J., Frank, T. D., Birgenheier, L. P., Niemeier, D., Fielding, C. R. and Rygel, M. C., 2007. CO2-Forced Climate and Vegetation Instability During Late Paleozoic Deglaciation, Science, 315(5808): 87-91.

MORROW, J.R., SANDBERG, C.A., MALKOWSKI, K., JOACHIMSKI, M.M., 2009. Carbon isotope chemostratigraphy and precise dating of middle Frasnian (lower Upper Devonian) Alamo Breccia, Nevada, USA. Palaeogeography, Palaeoclimatology, Palaeoecology 282: 105–118.

MUNNECKE, A., SAMTLEBEN, C., AND BICKERT, T., 2003. The Ireviken Event in the lower Silurian of Gotland, Sweden – relation to similar Palaeozoic and Proterozoic events. Palaeogeography, Palaeoclimatology, Palaeoecology, 195(1-2): 99-124.

MYROW, P. M., STRAUSS, J. V., CREVELING, J. R., SICARD, K. R., RIPPERDAN, R. SANDBERG, C. A. AND HARTENFELS, S., 2011. A carbon isotopic and sedimentological record of the latest Devonian (Fammenian) from the Western U. S. and Germany. Palaeogeography, Palaeoclimatology, Palaeoecology 306: 147-159.

MYROW, P. M., HANSON, A., PHELPS, A. S., CREVELING, J. R., STRAUSS, J. V., FIKE, D. A. AND RIPPERDAN, R. L., 2013. Latest Devonian (Famennian) global events in western Laurentia: Variations in the carbon isotopic record linked to diagenetic alteration below regionally extensive unconformities. Palaeogeography, Palaeoclimatology, Palaeoecology 386: 194-209.

MYROW, P. M., RAMEZANI, J., HANSON, A. E., BOWRING, S. A., RACKI, G. AND RAKOCIŃSKI, M, 2014. High-precision U-Pb age and duration of the latest Devonian (Famennian) Hangenburg event, and its implications. Terra Nova, 26(3): 222-229.

PISARZOWSKA, A. AND RACKI, G., 2012. Isotopic chemostratigraphy across the Early-Middle Frasnian transition (Late Devonian) on the South Polish carbonate shelf: A reference for the global punctata Event. Chemical Geology, 334: 199-220.

QIE, W. -K., ZHANG, X.-H., DU, Y. –S. AND ZHANG, Y., 2010. Lower Carboniferous carbon isotope stratigraphy in South China: Implications for the Late Paleozoic glaciation. Science China Earth Sciences, 54(1): 84-92. Saltzman, M.R., González, L. A. and Lohmann, K. C., 2000. Earliest Carboniferous cooling step triggered by the Antler orogeny? Geology, 28: 347-350.

SALTZMAN, M. R., 2002. Carbon and oxygen isotope stratigraphy of the Lower Mississippian (Kinderhookian-lower Osagean), western United States: Implications for seawater chemistry and glaciation. Geological Society of America Bulletin, 114 (1): 96-108.

SALTZMAN, M.R., 2003. The Late Paleozoic Ice Age: Oceanic gateway or pCO_2? Geology, 31: 151-154.

SALTZMAN, M.R. AND THOMAS, E., 2012. Chapter 11 Carbon Isotope Stratigraphy in Gradstein, F.M., Ogg, J.G., Schmitz, M. and Ogg, G. (eds) The Geologic Time Scale: 207-232. Elsevier B.V.

SCHOLLE, P. A. AND ARTHUR, M. A., 1980. Carbon Isotope Fluctuations in Cretaceous Pelagic Limestones: Potential Stratigraphic and Petroleum Exploration Tool. The American Association of Petroleum Geologists Bulletin, 64(1): 67-87.

ŚLIWINSKI, M. G., WHALEN, M. T., NEWBERRY, R. J., PAYNE, J. H. AND DAY, J. E., 2011. Stable isotope ($\delta^{13}C_{carb}$ and org, $\delta^{15}N_{org}$) and trace element anomalies during the Late Devonian 'punctata Event' in the Western Canadian Sedimentary Basin. Palaeogeography, Palaeoclimatology, Palaeoecology, 307: 245-271.

VEEVERS, J. J. AND POWELL, M., 1987. Late Paleozoic glacial episodes in Gondwanaland reflected in transgressive-regressive depositional sequences in Euramerica: Geological Society of America Bulletin, 98: 475-487.

YANS, J., CORFIELD, R. M., RACKI, G. AND PREAT, A., 2007. Evidence for perturbation of the carbon cycle in the Middle Frasnian punctata Zone (Late Devonian). Geological Magazine, 144(2): 263-270.